Preparation of Ecological Refractory Bricks from Phosphate Washing By-Products

Mariem Hassen , Raja Zmemla , Mouhamadou Amar * , Abdalla Gaboussa , Nor-edine Abriak , Ali Sdiri

Posted Date: 12 June 2025

doi: 10.20944/preprints202506.1064.v1

Keywords: phosphate sludge; characterization; mining byproducts; valorization; fired bricks; geopolymerization

 doi:10.20944/preprints202506.1064.v1

Article

Preparation of Ecological Refractory Bricks from Phosphate Washing by-Products

Mariem Hassen [1], Raja Zmemla [2], Mouhamadou Amar [3,*], Abdalla Gaboussa [4], Nordine Abriak [3] and Ali Sdiri [5]

[1] National School of Engineers of Sfax
[2] Laboratory of Environmental Engineering and Ecotechnology, ENIS
[3] IMT Nord Europe
[4] Higher Institute of Technological Studies of Gafsa
[5] Ecole Nationale d'Ingénieurs de Sfax, Sfax, Tunisia
* Correspondence: mouhamadou.amar@imt-nord-europe.fr

Abstract: This research is to assess the potential use of phosphate sludge from the Gafsa (Tunisia) phosphate laundries as an alternative raw material for the manufacture of ecological refractory bricks. Feasibility was evaluated through comprehensive physico-chemical and mineralogical characterizations of the raw materials using X-ray diffraction (XRD), X-ray fluorescence (XRF), Fourier transform infrared spectroscopy (FTIR), and thermal analysis (TGA-DTA). Bricks were formulated by substituting phosphate sludge with clay and diatomite, then activated with potassium silicate solution to produce geopolymeric materials. Specific formulations showed remarkable mechanical performances of approximately 7 MPa to 26 MPa, highlighting the importance of composition and minimal water absorption value of approximately 17.8% and 7.7%. The thermal conductivity of the bricks was found to be dependent on the proportions of diatomite and clay, reflecting their insulating potential. XRD analysis indicated the formation of an amorphous aluminosilicate matrix, while FTIR spectra confirmed the development of new chemical bonds characteristic of geopolymerization. Thermal analysis revealed good stability of the materials, with mass losses mainly related to dehydration and dehydroxylation processes. Environmental assessments showed that most samples are inert or non-hazardous, though attention is required for those with elevated chromium content. Overall, these findings highlight the viability of incorporating phosphate sludge into fired brick production, offering a sustainable solution for waste valorization in accordance with circular economy.

Keywords: phosphate sludge; characterization; mining byproducts; valorization; fired bricks; geopolymerization

Introduction

Phosphate mines generate millions of tons of waste rock in open-pit mining [1]. Furthermore, during phosphate ore processing, fluorapatite is separated from associated gangue minerals through a combination of successive mineral processing steps including crushing/sieving, washing and flotation. These operations produce large volumes of tailings, known as phosphate slurry, which are dumped into large surface ponds, while waste rock is dumped into the mine. In general, the mining industry is facing many environmental challenges resulting from the huge quantities of waste that mines engender, such as waste rocks, concentrator tailings, and phosphate sludge. These wastes are deposited or stockpiled within the mine site and constitute a potential source of pollution because of their chemical characteristics and grain size[2].

Tunisia, with its large phosphate reserves, is the fifth largest producer of phosphates in the world, which have been mined for more than a century. Nationwide phosphate reserves are estimated at 325 billion tons. These phosphates are transformed into fertilizers for agriculture. The

 doi:10.20944/preprints202506.1064.v1

main phosphate deposits are divided into 3 areas: The Northern phosphate area (Srâa El -Ouertane and Kalaâ-Khasba), the phosphate area of the Center (Chérahil, Maknassy), and the phosphate area of the South (Gafsa). These three areas represent one of the most important phosphate complexes in the world. Thus, the Tunisian phosphate sector, represented by the Phosphates Company of Gafsa (CPG) and its subsidiary GCT (Tunisian Chemical Group), has stopped growing. represents a large part of the economic activity of Tunisia 4.5% of GDP [3]. Tunisian natural phosphate is a rock formed approximately 50 million years ago (Eocene), characterized by a beige color, a sandy texture, and a soft consistency, with high porosity. Its microcrystalline structure is composed of carbonated fluorapatite.

This intense mining activity related to natural phosphate beneficiation generates large amounts of sludge. In Tunisia for instance, 11 million metric tons per year of phosphate sludge were deposited in 2011 [3]. However, this activity, like any mining activity, generates environmental damages related to dust, wastewater, and atmospheric emissions from ore processing plants, which are not without consequences for water resources, wildlife, flora, and human health: air pollution, water, and soil pollution, chronic diseases, degradation of the vegetation cover and wildlife habitat area [2]. Recently, with the growing environmental awareness and regulation incentives, mining companies are looking for sustainable and feasible solutions to minimize the high amounts of waste. Consequently, many promising eco-friendly solutions have been established by numerous researchers [4]. Nowadays, several industrial and mining wastes have been studied for their potential use as alternative materials. Although the mining industry still considers most of its waste as materials without any value, recent trends favored by incentive legislation showed that the potential mine waste reuse could be beneficial in many cases, especially when they are proven not acid-generating. Building materials are supposed to be the utmost efficient way to consume these substantial amounts of waste generated every day [4].Therefore, the recycling of mining waste as raw materials for the construction industry allows the reduction of the quantity of this waste and also the preservation of natural resources [5]. For Obenaus-Emler et al[6]alkali-activated materials can be made from mine tailings, geopolymers[7] or in the Preparation of concrete blocks using purified tailing [8]. More recently, Boutaleb et al. [9,10] demonstrated that phosphate mine tailings improve the mechanical properties of ceramic tiles. They used industrial mine tailings at a rate of 33% in formulas based on local clays for ceramic material manufacturing. Bricks with up to 30% phosphate sludge exhibited acceptable mechanical properties, meeting industry standards. Environmentally, incorporating sludge reduced clay consumption and waste, while increasing open porosity and water absorption, with 50% sludge resulting in 52% porosity and 32% water absorption [11]. For Inabi et al. [12] the bricks manufactured using phosphate washing sludge exhibit robust mechanical performance, low embodied energy, excellent insulation, and thermal properties. Also, it was demonstrated that Bricks manufactured with 2.5% phosphate sludge demonstrated approved compressive strength and met environmental standards, classified as non-inert materials [13]. Valorization of tailings could be a promising alternative not only to reduce their potential environmental impacts but also to create a path for an eco-commercial profit by making a good business opportunity.

Given the significant environmental challenges posed by the accumulation of phosphate washing by-products in the Gafsa-Metlaoui region, this research aims to explore a sustainable pathway for their valorization through the development of ecological refractory bricks. By systematically characterizing the physical, chemical, and mineralogical properties of local phosphate sludge and evaluating its performance as a primary precursor-alone and in combination with natural clay and diatomite-this study investigates the feasibility of producing high-quality geopolymer bricks activated with potassium silicate. The resulting materials are rigorously assessed for mechanical strength, water absorption, thermal conductivity, and environmental safety to ensure compliance with construction standards. Ultimately, this approach offers a promising solution for transforming mining waste into value-added construction materials. Aligning with circular economy principles and contributing to both environmental protection and resource efficiency in the region.

 doi:10.20944/preprints202506.1064.v1

Mining Site

In Tunisia, the GPG oversees the processing of phosphate ores in ten washing stations, each discharging approximately 284,000 m^3 of sludge into the rivers of the Gafsa region [5]. To optimize water recovery and reduce the volume of sludge for disposal, the GPG has implemented underground pipelines to transfer sludge from the washing stations to storage basins. By 2001, the accumulated sludge in these basins exceeded 11 million m^3, with over 90% not reaching the residue basins but being dispersed outside through an artificial river system. Between 1998 and 2011, around 2.5 million tons of sludge were annually discharged into the Thelja, Sebseb, and El Malah rivers [3].

Our study area is located in the Gafsa mining basin, a region highly impacted by phosphate mining activities. This basin encompasses several key sites critical to understanding the environmental effects of mining sludge disposal. Specifically, we focused on three sampling zones (Figure 1): Métlaoui (also known as Thelja), the first city in the basin and a central hub for mining operations; Redeyef, another major mining town within the basin; and Oued Etfal, situated approximately 20 km from Gafsa along the regional road R201 connecting Gafsa to Moulares.

Figure 1. Study Area and Locations of the Three Sampling Sites.

Materials and Methods

Materials Used

Sludge samples were collected from washing station 2 in Métlaoui Gafsa after the flocculation process to characterize these by-products in the context of our ongoing study.

The materials employed in this study encompassed a selection of constituents: phosphate waste sludge (PWS), natural clay from Oued Tfal near Gafsa (20 km from Gafsa), diatomite from the Nagues quarry in Redeyef, corresponding to the interlayer between layers 6 and 7 of the phosphate series, and alkaline silicate (ALK) (with the product name Geosil). The phosphate sludge, sourced from industrial waste, served as a key precursor after calcination at 850°C. The kaolinic clay underwent thermal transformation at 700°C, acting as the primary geopolymer precursor and providing aluminosilicates necessary for the chemical reaction. Diatomite was calcined at 750°C to enhance its reactivity and stability. Potassium silicate was employed to initiate geopolymerization, while ensuring the formation of a durable aluminosilicate matrix. This combination of materials aimed to produce sustainable refractory bricks with improved mechanical and thermal properties.

 doi:10.20944/preprints202506.1064.v1

Mix Proportioning

The use of washing phosphate sludge (WPS), kaolinitic clay (KC), and diatomite (D) as precursors in alkali-activated geopolymer binders promotes sustainable construction practices by repurposing industrial and mining waste. These materials are abundantly available in regions like Gafsa, Tunisia, where phosphate mining generates significant sludge byproducts, while (KC) and (D) are locally sourced natural minerals. Previous studies have limited WPS substitution in refractory materials to 50% due to its lower reactivity[7,14,15] However, this research expands the substitution range from 50% to 100% to optimize waste valorization. The formulations GBM (PS + KC), GBD (WPS + D), and GBDM (WPS + KC + D) (Figure 1) were designed using potassium silicate (K_2SiO_3) as the alkaline activator, with its concentration fixed to 15% of the binder weight, as derived from preliminary trials and literature.

Mixes Preparation Protocol

The refractory geopolymer bricks were formulated by combining washing phosphate sludge, kaolinitic clay, and diatomite in varying proportions, following a systematic mixing protocol adapted to ensure optimal homogeneity and performance. The preparation process consisted of several structured steps. First, the raw materials were weighed, and the dry components (PS, KC, and D) were mixed for 5 minutes to achieve a uniform blend. Subsequently, the potassium silicate solution was gradually added over 10 minutes while maintaining continuous mixing to ensure even distribution and activation of the binders.

The fresh geopolymer bricks were then poured into cylindrical molds (Ø50 mm × 50 mm) and compacted to achieve optimal density. The molds were sealed immediately to initiate the curing process, allowing the geopolymer matrix to mature under ambient conditions for 72 hours. Finally, the samples were oven-dried at 105°C for 24 hours to remove residual moisture and enhance their mechanical properties (Figure 2).

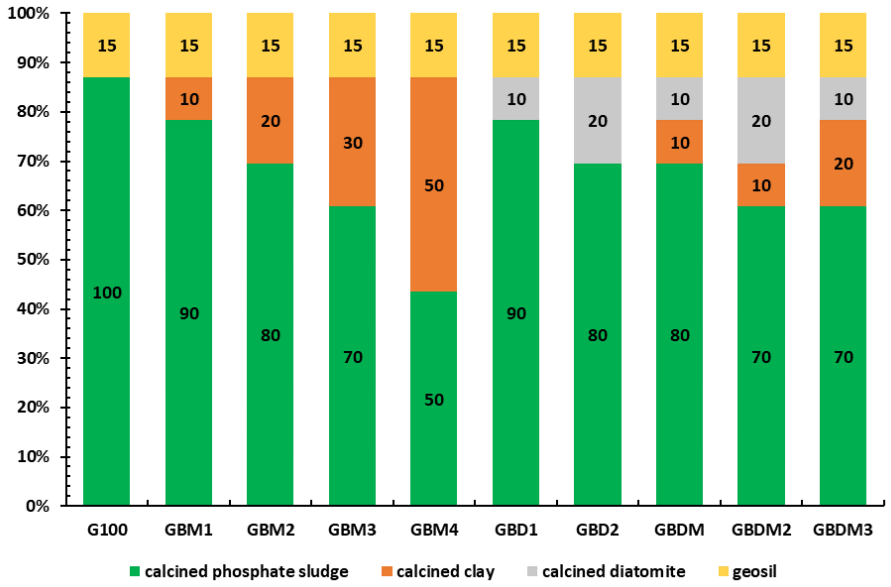

Figure 2. Brick formulation composition.

This meticulous procedure ensured consistent mixing, compaction, and curing, which are critical factors in evaluating the structural integrity and durability of geopolymer-based refractory bricks.

 doi:10.20944/preprints202506.1064.v1

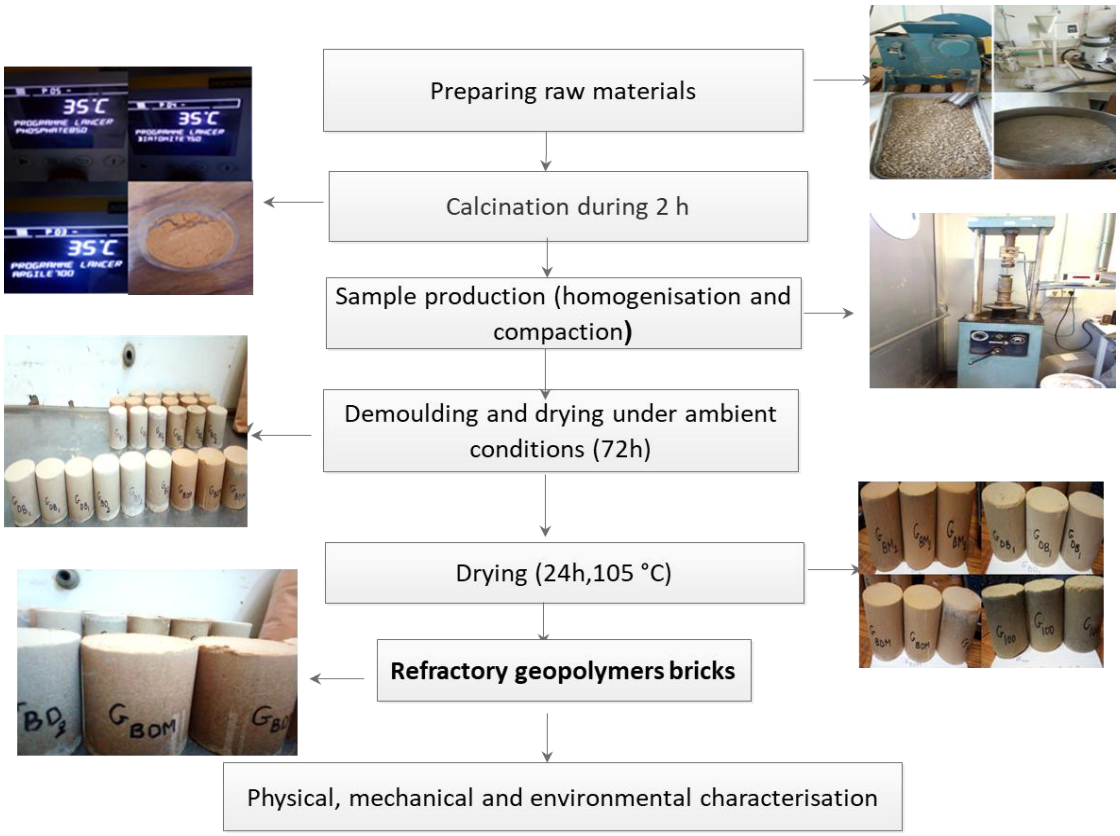

Figure 3. Simplified diagram illustrating refractory geopolymers bricks making.

Experimental Methods

Material Characterization

The raw materials were characterized using various analytical techniques to determine their chemical and physical properties. The analyses included:

- **X-ray fluorescence (XRF)** for bulk chemical composition;
- **Loss on ignition (LOI)** to assess volatile content;
- **Particle size distribution (PSD)** to determine granulometry.

Phase identification and structural information were obtained through:

- **X-ray diffraction (XRD)** using a Bruker D2 diffractometer equipped with a Cu-Kα radiation source (λ = 1.5406 Å);
- **Fourier-transform infrared spectroscopy (FTIR)** performed with a Thermo Scientific Nicolet iS20 instrument.

These analyses provided detailed insights into the mineralogical composition and microstructure of the raw materials and resulting brick specimens.

Mechanical Testing

Compressive strength tests were conducted on cylindrical specimens (Ø50 mm × 50 mm) using an INSTRON 5500 R universal testing machine, following the NF EN 196-1 standard. For each brick formulation, three replicate specimens were tested to ensure reproducibility. Additional mechanical tests were also performed on fired bodies to evaluate the influence of thermal treatment.

 doi:10.20944/preprints202506.1064.v1

Water Absorption

Water absorption (W_d) was measured in accordance with the NF P51-302 standard. Three brick specimens per formulation were dried to constant mass (M_d), cooled to room temperature (20 °C), and immersed in water for 24 hours. After immersion, excess surface water was removed and the wet mass (M_s) was recorded. The water absorption was calculated as (Equation (1)):

$$W_S(\%) = \frac{M_S - M_d}{M_d} * 100 \quad (1)$$

Thermal Conductivity

Thermal conductivity measurements were carried out using the transient plane source (TPS) method with a **Hot Disk** apparatus. A resistive sensor functioning as a planar heat source was positioned between two identical pellets. The temperature rise resulting from heat dissipation was monitored and analyzed using dedicated software to calculate thermal conductivity. The measurement is based on Fourier's law of thermal conduction (Equation (2)):

$$q(r,t) = -k\Delta T(r,t) \quad (2)$$

where q represents the heat flux density, k the thermal conductivity, and $\Delta T(r,t)$ the temperature gradient.

Thermogravimetric Analysis (TGA)

Thermogravimetric analysis was performed using a NETZSCH STA 409 instrument under a nitrogen atmosphere. The heating program involved a constant rate of 10 °C/min, from 40 to 1000 °C. This test provided information on the thermal stability and decomposition behavior of the samples.

Chemical and Environmental Analysis

Trace element concentrations were determined via **inductively coupled plasma atomic emission spectrometry (ICP-AES)**. Additionally, the concentrations of water-soluble ions such as sulfates, chlorides, and fluorides were quantified by **ion chromatography**. The environmental behavior of the bricks was assessed through leaching tests in accordance with applicable protocols.

Durability Assessment

The durability of the bricks was evaluated using an **efflorescence test**, following the NF EN 772-5 standard. This test assessed the potential for formation of surface crystalline deposits resulting from the migration of soluble salts.

Experimental Protocol

All tests were carried out at the *IMT Nord Europe Center for Education, Innovation and Research*. Unless otherwise stated, six specimens were prepared and tested for each formulation, in compliance with the relevant technical standards for mechanical, thermal, and physical characterization.

Results and Discussion

Raw materials Characterization

Physical Characterization

The sludges from the Gafsa phosphate washery exhibit distinct granulometric characteristics, with over 90% of particles being smaller than 200 µm (Table 1). Detailed analysis reveals a bright sandy texture, without the presence of particles exceeding 90 micrometers, indicating an absence of clay components. The particle size distribution, characterized by a conformity coefficient of 5 and a uniformity coefficient of 1.58, suggests marked heterogeneity in the soil composition but also a relative uniformity in particle sizes within the sample. These findings underscore the need for careful

 doi:10.20944/preprints202506.1064.v1

management of phosphate sludges to minimize their potential environmental impact. The density of the sludge was 2.85 g/cm^3 and the loss on ignition was 6.23%.

Table 1. physical characteristics of sludge.

Particle Diameter (μm)	**Diameter**	**Volume %**
D10	10	1.2
D25	25	6.0
D50	50	42.7
D75	75	136.7
D90	90	178.4
Bulk Density (γ_s)		2.85 g/cm^3
Loss on Ignition (W_LOI)		6.23 %
Water Demand (D_water)		0.243 %

Mineralogical Characterization

Raw Materials

X-ray Diffraction (XRD) analysis was conducted to determine the mineralogical composition of the raw materials used in this study, revealing that the phosphate sludge (Figure 4) primarily consists of apatite (fluorapatite $Ca_{10}(PO_4)_6F_2$ or carbonated apatite) as the predominant crystalline phase, with minor components of calcite ($CaCO_3$), quartz (SiO_2), and clay minerals, consistent with previous research[5] and [16], with the XRD patterns suggesting that the clay, calcite, and quartz phases are predominantly associated with the exogangue components of the sludge, while their interference with the fluorapatite peaks may stem from their presence as endogangue constituents; the XRD patterns for the raw natural clay (Figure 4) reveal a complex mineralogical composition, confirming its heterogeneous nature and detecting the presence of illite, kaolinite, hematite, dolomite, quartz, and calcite, consistent with the findings reported) with those reported by Bouaziz in a similar study of natural clay mineralogy [17] in a similar study of natural clay mineralogy; and the XRD spectra for raw diatomite (Figure 6) reveal its composition primarily consists of amorphous silica (SiO_2) phases, along with crystalline quartz and calcium carbonate (calcite and dolomite), also identifying trace amounts of clay minerals and feldspars (albite, orthoclase).

 doi:10.20944/preprints202506.1064.v1

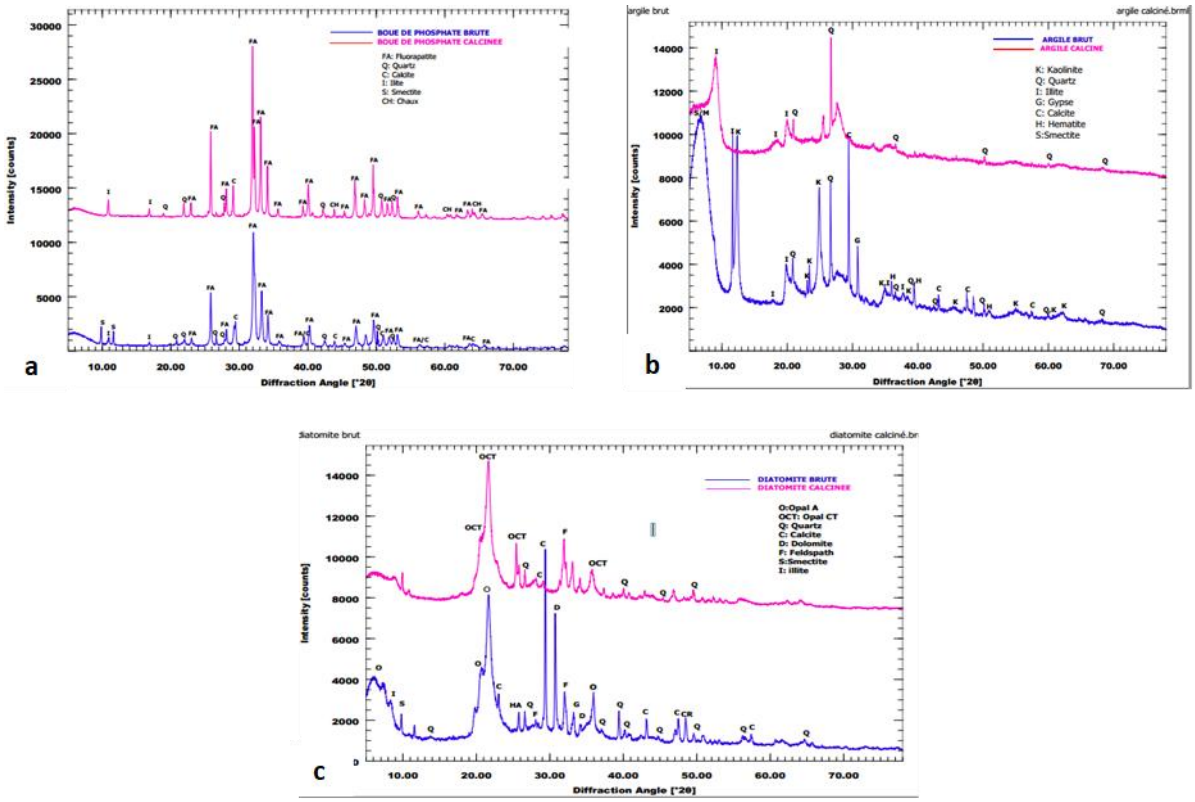

Figure 4. Crystalline phases present in raw phosphate sludge (a); raw natural clay (b) and in raw diatomite (c).

Effect of Thermal Treatment on Raw Materials

Thermal treatment of raw materials induced notable changes in their mineralogical compositions. For phosphate sludge, calcination led to sharper XRD peaks, indicating improved apatite crystallinity, and the disappearance of calcite peaks, signaling its thermal decomposition into calcium oxide, while quartz remained stable (Figure 4). In natural clay, calcination transformed kaolinite into amorphous metakaolinite, evidenced by a broad peak at 27.9° 2θ, with illite, hematite, and quartz peaks persisting (Figure 4). Finally, calcination of diatomite promoted partial recrystallization, reduced clay impurities and calcite peaks, and caused structural rearrangements evident in cristobalite and quartz peak variations (Figure 6).

Fourier Transform Infrared (FTIR) Spectroscopy

Fourier Transform Infrared was employed to reveal key functional groups and the impact of thermal treatment. The FTIR spectrum of raw phosphate sludge exhibited a broad absorption band between 3000 and 3600 cm^{-1}. That is indicative of significant water content, with the region between 1000 and 1200 cm^{-1} suggesting the presence of phosphate groups (PO_4^{3-}) and 1400-1600 cm^{-1} hinting at carbonates or organic matter. After calcination, the water band diminished, phosphate groups became more defined and changes below 800 cm^{-1} pointed to crystalline restructuring (Figure 5). Similarly, FTIR analysis of raw clay from Oued Tfal showed a broad band in the 3700-3000 cm^{-1} region, characteristic of O-H stretching vibrations from water and hydroxyl groups within clay minerals, consistent with [NO_PRINTED_FORM] [17]. This band attenuated after calcination, while Si-O-Si bands initially located between 1000 and 1100 cm^{-1} transformed into a wider, less defined band. The bands associated with kaolinite, like Si-O-Al (<800 cm^{-1}) and Al-OH (915 cm^{-1}), disappeared, in agreement with Louati et al. [18], indicating dehydroxylation and the disruption of the silicate network. Finally, FTIR spectra of diatomite before calcination displayed a broad, intense band around 3400 cm^{-1}, attributed to O-H stretching vibrations from adsorbed water and silanol

 doi:10.20944/preprints202506.1064.v1

groups (Si-OH), and a peak at 1630 cm^{-1} corresponding to water bending; after calcination at 750°C, these bands nearly vanished, indicating the elimination of adsorbed and structural water, while the bands at 1000-1200 cm^{-1}, 800 cm^{-1}, and 460 cm^{-1} representing Si-O-Si stretching and bending vibrations. Zheng et al [NO_PRINTED_FORM] [19] showed that the band at 800 cm^{-1} became narrower and more continuous, suggesting an improved silica crystallinity, although the overall silica network structure was retained, aligning with the XRD results.

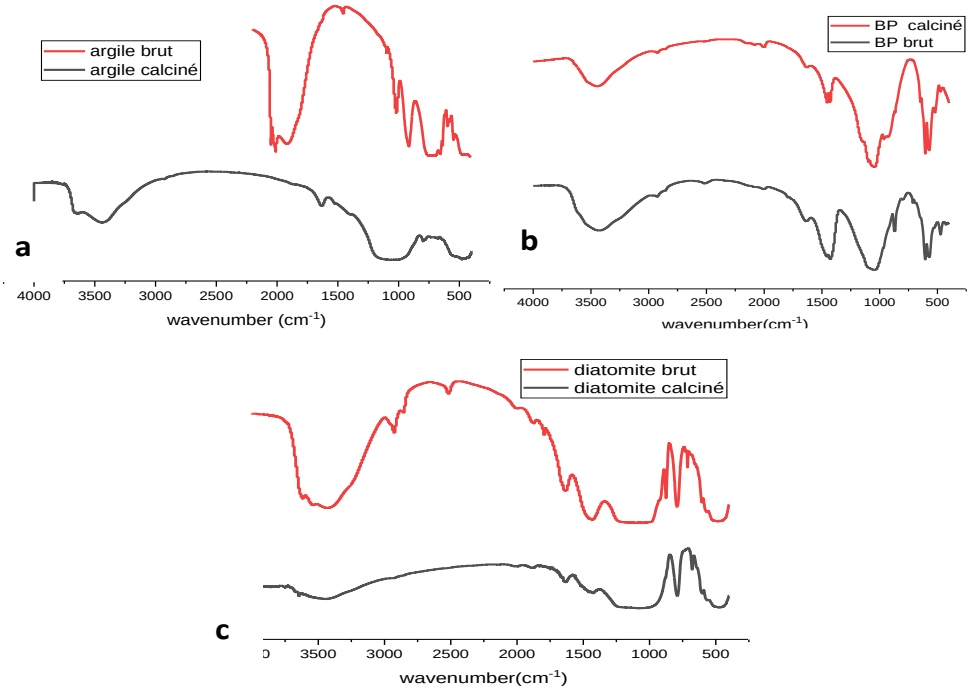

Figure 5. IRTF Spectrum of: (a) Natural and calcined phosphate sludge; (b) natural and calcined clay; (c) raw and calcined diatomite.

Thermogravimetric Test

Phosphate Sludge

the TGA of phosphate sludge reveals three main stages of mass loss visible in Figure 6:

- 200°C to 400°C: 7.4% loss, corresponding to the decomposition of organic matter. This is due to thermolyzing organic compounds in the sludge, like proteins, lipids, and carbohydrates.
- 400°C to 600°C: 1.3% loss, attributed to fluorapatite decomposition. This occurs through dehydration, transforming fluorapatite into hydroxyapatite.
- 600°C to 800°C: 1.5% loss, associated with calcite decomposition. This stems from the thermal breakdown of calcite into calcium oxide.

The total mass loss of 10.2% indicates a significant organic content in the phosphate sludge.

Here's an interpretation based on the mineral composition: 74% organic matter: decomposes between 200°C and 400°C.,13% fluorapatite: decomposes between 400°C and 600°C.and 15% calcite: decomposes between 600°C and 800°C.

 doi:10.20944/preprints202506.1064.v1

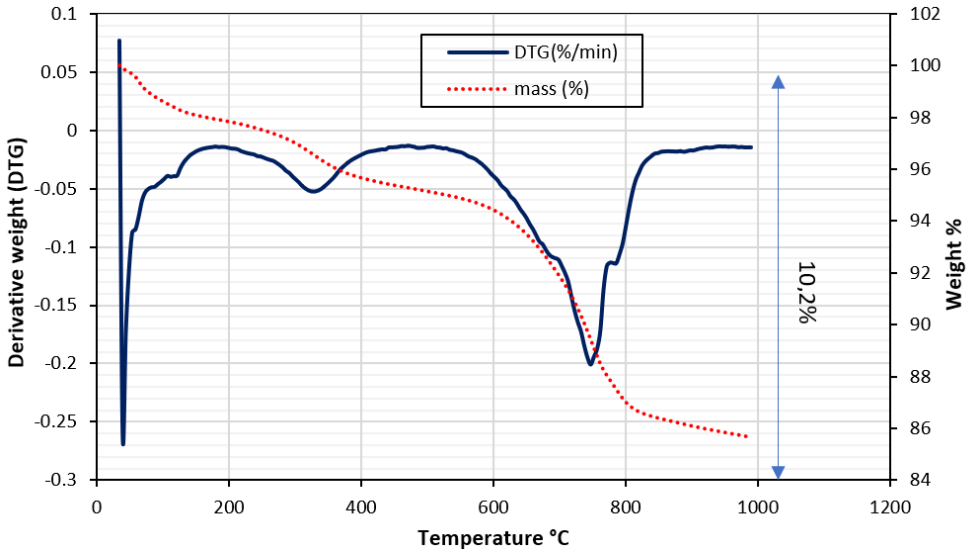

Figure 6. Thermogravimetric and differential thermogravimetric curves of phosphate sludge.

Natural Clay

The TG/DTG analysis reveals a thermal decomposition of the natural clay in several stages (Figure 7). Initially, a slight mass loss is observed up to approximately 200°C, likely due to the desorption of water or residual solvents from the material's surface. The most significant mass loss occurs between 400°C and 600°C, with a major peak on the DTG curve around 500°C (Figure 7). This mass loss corresponds to the dehydroxylation of kaolinite and the formation of metakaolin. The initial mass loss below 200°C can be attributed to the loss of water adsorbed by smectite and/or gypsum, while the slower mass loss above 600°C could correspond to the decomposition of carbonates (calcite) or structural transformations of other mineral phases present. The total mass loss observed over the entire temperature range is approximately 12%, reflecting the total amount of volatile materials or decomposable compounds, including water released during the transformation into metakaolin.

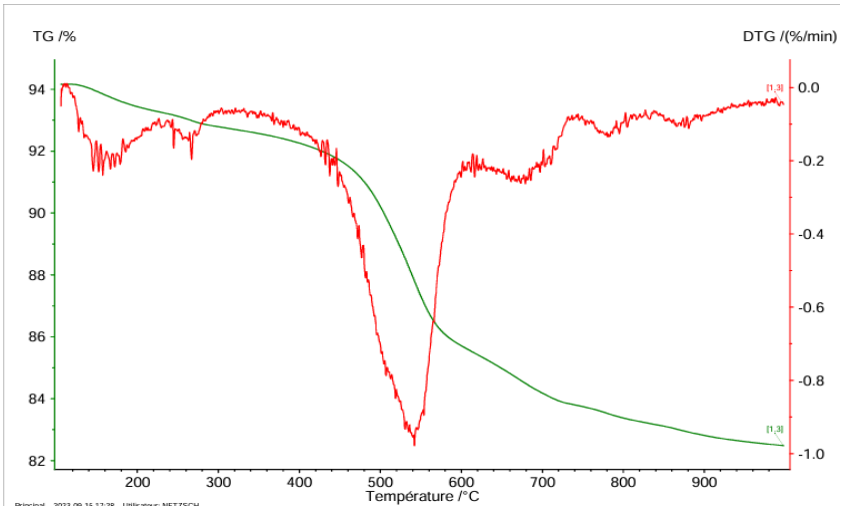

Figure 7. Thermogravimetric and differential thermogravimetric curves of natural clay.

Diatomite Mineral

The DTG thermograph reveals the presence of two endothermic peaks at around 90°C and 750°C, respectively. The first peak, which is associated with a mass loss of approximately 2 to4% at low temperature, is typical of diatomite, which is known for its high porosity and ability to physically adsorb water, a characteristic confirmed in the literature on natural diatomites [20]. The second

 doi:10.20944/preprints202506.1064.v1

endothermic peak, correlated with a mass loss of approximately 8%, can be attributed to the decarbonation of calcite (Figure 8). This would contribute to decreasing its thermal conductivity, thereby improving its thermal insulation capacity [20].

The continuous decrease of the TG curve below 800°C and the increase of the DTG curve after the 750°C peak may be due to an exothermic reaction. Thus the formation of compounds resulting from the destruction of diatomite. Alternatively, the mineralogical rearrangement of the siliceous phase following the transformation of opal-CT to opal-C is more ordered [21]. This phenomenon corresponds to recrystallization.

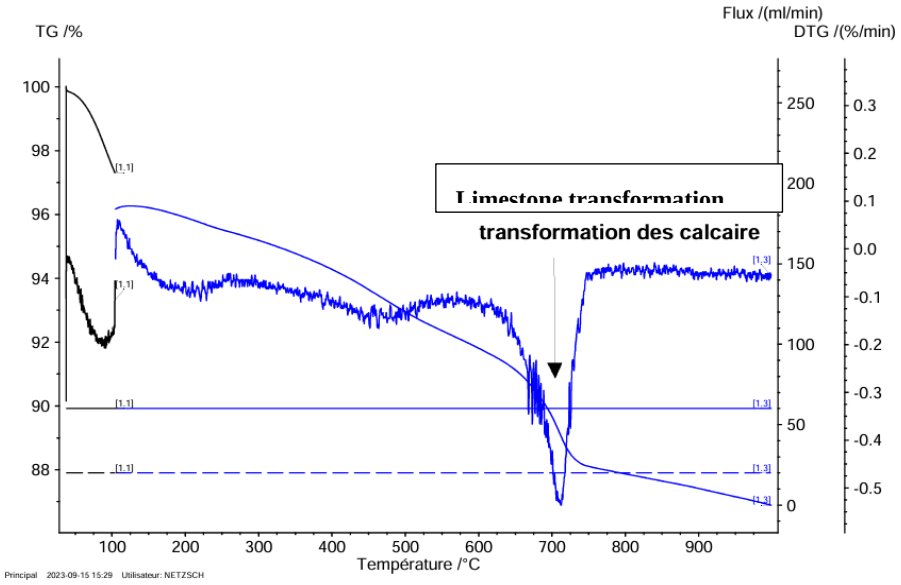

Figure 8. Thermogravimetric and differential thermogravimetric curves of diatomite.

Environmental Characterization of Raw Materials:

The environmental analysis of mining effluents from the phosphate washery, natural Clay and diatomite reveals concentrations of trace elements using Inductively Coupled Plasma Atomic Emission Spectrometry (ICP-AES). The detection limits for various elements indicate method sensitivity. While, most heavy metals such as As, Ba, Cd, Cu, Ni, Pb, Sb, and Zn are present at concentrations far below the regulatory limits for inert (ISDI) and non-hazardous (ISDND) waste (see Table 2). However, calcined phosphate sludge shows a significant increase in chromium (Cr) leaching (up to 79 mg/L), exceeding the ISDN D limit (10 mg/L) and even surpassing the hazardous waste threshold (ISDD, 70 mg/L). Molybdenum (Mo) and selenium (Se) also increase after calcination, sometimes exceeding the ISDI limits. Sulfate, chloride, and fluoride concentrations are generally high, especially in phosphate sludge, but remain below ISDND thresholds.

Table 2. heavy metals and anions of raw and calcined materials.

Elements	Phosphate sludge (mg/l)	Clay mineral	diatomite	Calcined clay	Calcined Phosphate sludge	Calcined diatomite	ISDI	ISDND	ISDD
As	<0.1	< 0.1	< 0.1	0,18	< 0.1	< 0.1	0.5	2	25
Ba	0.068	< 0.008	0,026	< 0.008	0,34	0,034	20	100	300
Cd	<0.009	< 0.009	< 0.009	< 0.009	< 0.009	< 0.009	0.04	1	5
Cr	0.025	< 0.004	0,01	15	79	17	0.5	10	70
Cu	<0.02	< 0.02	< 0.02	< 0.02	< 0.02	< 0.02	2	50	100
Mo	0.55	0,18	2,0	0,88	7,3	6,1	0.5	10	30
Ni	<0.05	< 0.05	0,076	< 0.05	< 0.05	< 0.05	0.4	10	40

 doi:10.20944/preprints202506.1064.v1

Pb	<0.03	< 0.03	< 0.03	< 0.03	< 0.03	< 0.03	0.5	10	50
Sb	<0.06	< 0.06	< 0.06	0,06	0,34	< 0.06	0.06	0.7	5
Se	0.088	0,32	0,48	0,23	5,8	0,99	0.1	0.5	7
Zn	0.63	0,81	0,91	0,82	0,96	0,61	4	50	200
Sulfates	4760	644	724	353	450	1350	1000	20000	50000
Chlorures	386	487	80	259	70	13,5	800	15000	25000
Fluorures	14	2,0	1,5	2,1	13,4	1,8	10	150	500

Geopolymer Bricks Characterization

Compressive Strength

The compressive strength of geopolymer bricks is an important property in material formulation. Higher resistance to compressive force also suggests a much better microstructure and improved durability properties for the bricks. Figure 9 shows the compressive strength of the developed bricks. As seen, the binary mixture GBM1 (90% calcined phosphate sludge and 10% calcined clay) achieved a remarkable strength of 25.9 MPa, significantly surpassing the 17.8 MPa observed for the G100 formulation (100% calcined phosphate sludge) due to enhanced geopolymerization from reactive aluminosilicates [15,7]). This result shows the efficacy of controlled clay addition in boosting mechanical properties. While higher clay proportions decreased strength (down to 6.8 MPa), the initial benefit of 10% substitution demonstrates a key threshold for maximizing performance. Ternary mixtures (GBDM) and diatomite-based formulations (GBD) exhibited moderate strengths (11.4–15.9 MPa), suggesting their suitability for applications prioritizing thermal insulation over extreme mechanical demands [22]. The study confirms that strategic clay incorporation can significantly elevate geopolymer performance for refractory applications.

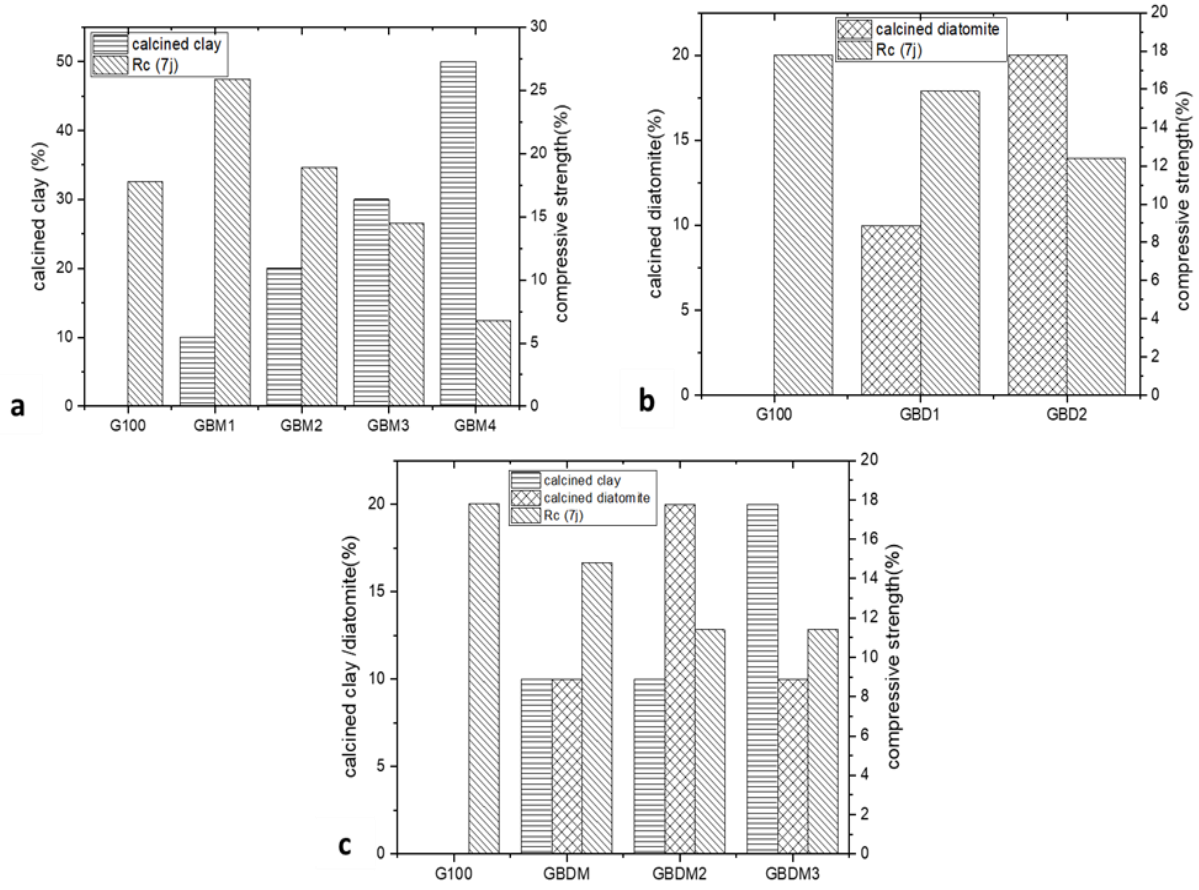

Figure 9. Compressive strength test results.

 doi:10.20944/preprints202506.1064.v1

Water Absorption

Low water absorption is desirable for refractory bricks, as it helps to reduce the risk of cracking and delamination. A recent study examined the influence of formulation composition on the water absorption of refractory bricks. Figure 10 shows that compositions with 100% calcined phosphate (G100) exhibit the lowest water absorption (~8%), indicating a dense microstructure with enhanced water resistance, slightly below values reported by [5]. Additives like diatomite (GBD series) and clay (GBM series) increase absorption up to 17% (GBDM3/GBM4), attributed to diatomite's inherent porosity and clay's post-calcination structural changes [14]. Key formulations (G100, GBM1-GBM3) comply with NF-EN 772-21 standards (17–22% absorption for frost-resistant bricks), aligning with findings that waste-derived additives can stabilize absorption [23], highlighting the need for precise additive control to optimize durability.

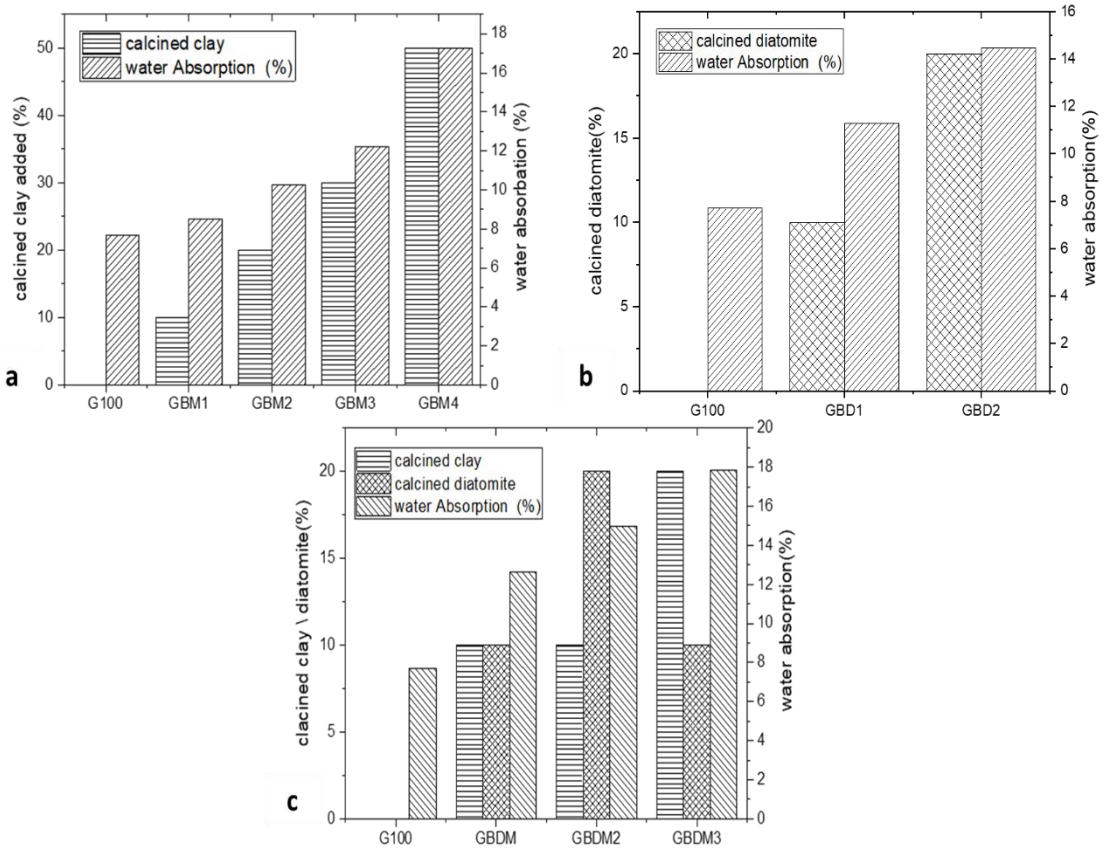

Figure 10. Water absorption of geopolymers bricks.

The following table compares selected results from other studies. That allows to compare deferent properties.

Table 3. Comparative studies of some geopolymers bricks formulations and results.

References	Valuation ways	Raw materials	Origine	Firing conditions	Water absorption (%)	Compressive strength (MPa)
[5]	Fired bricks	100% phosphate sludge	Tunisia Kef schfeir	Air drying for 24 h Oven drying at 60°C for 24 h Firing at 900°C, 1000°Cand 1100°C for 3 h (heating rate of 120°C	12.5-17.2	–

 doi:10.20944/preprints202506.1064.v1

[14]	Ceramics bricks	Indonesian sludge (Banten Province)	25-50% of phosphate sludge + kaolin	dried d in an oven at110°C for at least 24 hours. a heating rate of 5°C/min to 500°C, at 10°C/min from 500 to 925°C and at 15°C/min from 925°C	>30.23	> à 25
[16]	Ceramics products	Tunisian phosphate Kef eddour	0-50% phosphate sludge +kaolin	dried at 105 ° C for 24 h. The dried pellets were heated at 900, 1000 and 1100 °C for up to 2 h	–	–
[24]	Ceramics industries	Marrocan sludge	0-100% sludge+ 0-100% clay	heating ramp 5 ◦C/min up to the selected firing temperature (600, 900, 1000, 1100, and 1120 ◦C) 2h dwell time at the temperature selected		
[25]	Geopolymer	Marroc phosphate industry	alkaline solution, metakaolin-in and thermally untreated phosphate sludge (UPS)(of50%)	liquid to solid ratio of L/S=1.2. left drying at 60°C for 24 h. hardened matrices for 28 days	–	28.05-46.83
[26]	geopolymer	Fly ash came from the heat and power plant in Skawina (Poland), the metakaolin came from the Czech Republic and the diatomite came from the Jawornik Ruski	Fly ash (FA) + metakaolin (MK) + **1–5% diatomite**.	alkaline solution consisted of technical sodium hydroxide flakes with aqueous sodium silicate (a ratio of 1:2.5 was used) and tap water	Not specified	15- 31.7
[15]	Geopolymer		Phosphate washing waste and alkaline solution	PPW calcined at 700°C or 900°C, activated with NaOH (7M) and sodium silicate		15-22
[27]	Geopolymer		geopolymers based on Fly ash or metakaolin,			20-70
[28]	Fired bricks	China	84% hematite tailings, fly ash and clay mixed with 12.5-15% of water	20–25 MPa,of forming pressure and a suitable firing temperature was ranged from 980 to 1030 C for 2 h	16.54–17.93%	20.03–22.92 MPa
[29]	Hybrid brick	India	70-90 % clay + 5-15% ceramic waste powder + 5-15% bagasse ash.	The bricks were cast using moulds without any pressure being applied to them. In India, the bricks were left to dry in the sun for two days at a temperature of 35 to 40 °C. For an 800 ºC firing	11.4%-18 %	20-27.2

 doi:10.20944/preprints202506.1064.v1

Current Study	Geoploymer	Phosphate washing byproduct	50-100% phosphate washing byproduct + (10-50% calcined clay (GBM)/10-20% Calcined diatomite (GBD)/calcined diatomite +calcined clay (GBDM)) + potassium silicates solution	materials were calcined at 700°C; 750°C and 800°C, activated with potassium silicate solution then pressed, cured at ambient temperature for 72 hours, and oven-dried at 105°C for 24 hours	7.7-17.8% 7-26 MPa

Thermal Conductivity

The study of thermal conductivity in refractory bricks highlights significant trends influenced by composition. The G100 formulation (100% phosphate sludge) exhibits the highest thermal conductivity (0.55 W/m·K) (see Figure 11). Incorporating calcined diatomite (GBDM series) reduces conductivity to 0.38 W/m·K, while clay additions (GBM series) yield intermediate values (~0.50 W/m·K). These results align with the study of Bories et al. [30], who reported conductivity around 0.53 W/m·K for bio-based porous agents in fired clay bricks, and Phonphuak et al. [31] have reached lower conductivity (0.22–0.47 W/m·K) using sawdust, albeit with higher porosity (22.8–32.4%) [31]. This proves the critical role of pore agent type and quantity in modulating thermal and structural properties. Compared to commercial dense (1.0–2.0 W/m·K) and insulating (0.2–0.8 W/m·K) refractory bricks [30], the formulations developed in this study fall within the insulating range (0.38–0.58 W/m·K). Notably, the use of local, sustainable materials reduces the carbon footprint.

 doi:10.20944/preprints202506.1064.v1

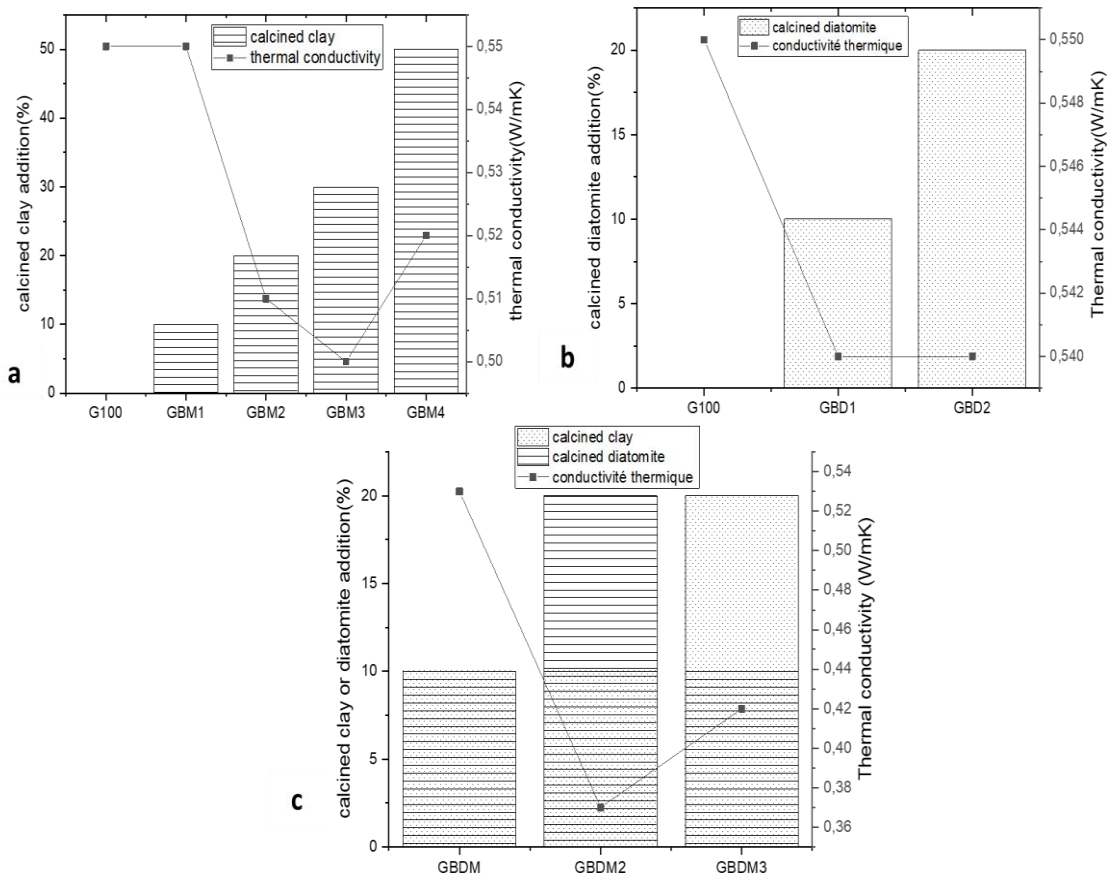

Figure 11. thermal conductivity of the studied samples.

X-Ray Diffraction Results

The X-Ray diffractograms of geopolymer formulations in Figure 12 revealed the mineralogical composition of consolidated materials. While geopolymers are generally considered amorphous materials by XRD, a broad hump centered around 20° to 35° (2θ) indicates the dissolution of SiO_4 and AlO_4 species and the formation of an amorphous phase compared to calcined clays, reflecting polycondensation reactions ([32] [33,17]). However, the significant intensity of crystalline peaks, particularly quartz, suggests limited reactivity and incomplete dissolution of raw materials ([34,35]). Compared to metakaolin-based geopolymers, which typically exhibit more complete amorphization [17], our materials show similarities to fly ash-based geopolymers, which often retain residual crystalline phases [36]. These crystalline phases may contribute to thermal stability, making the materials potentially suitable for refractory applications. Thus, while geopolymerization is evident, optimization of synthesis conditions is needed to enhance precursor reactivity and achieve improved performance for refractory uses.

 doi:10.20944/preprints202506.1064.v1

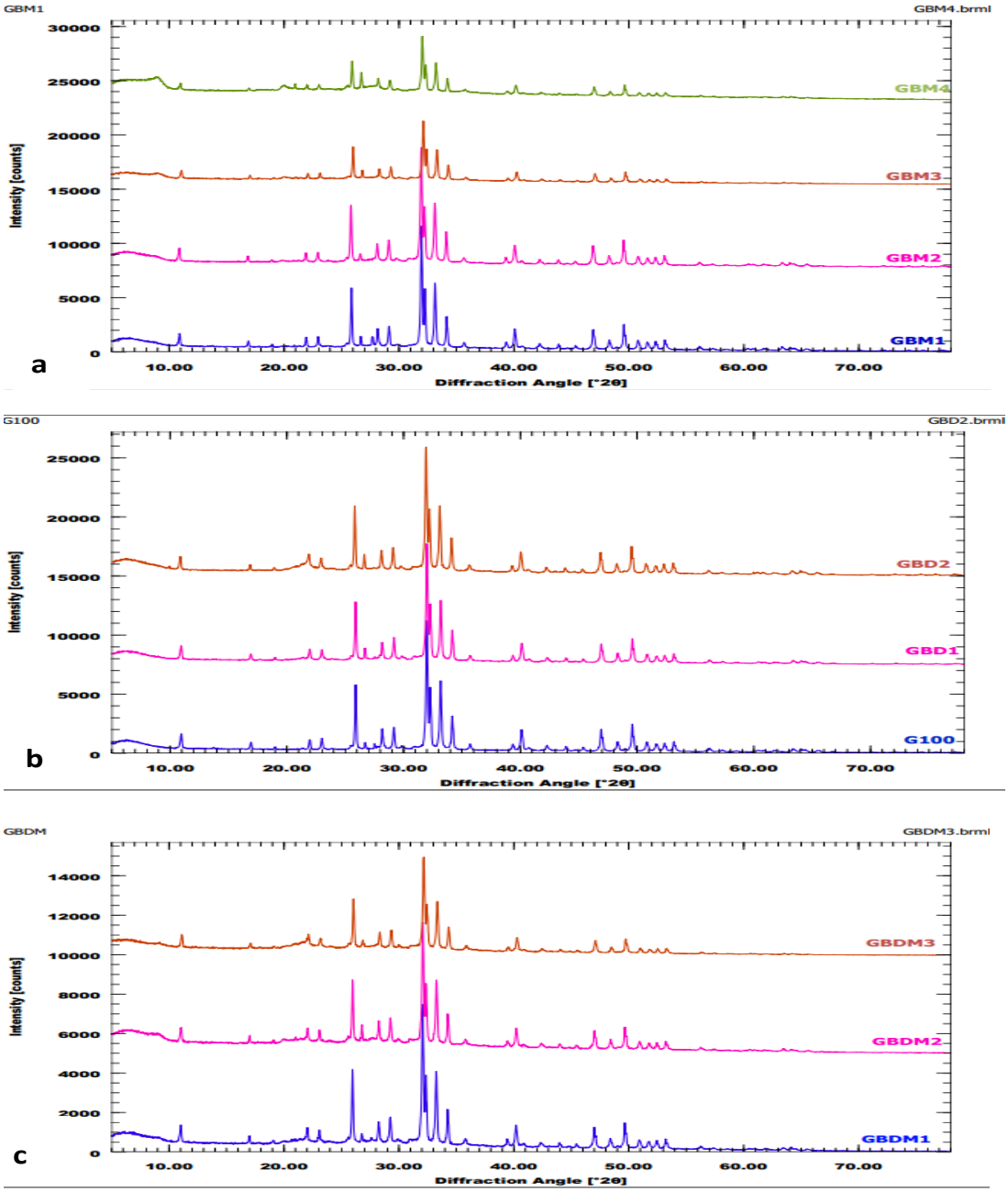

Figure 12. XRD patterns of the different geopolymers compositions/ (A): GBM series; (B): GBD series and (C): GBDM series.

FTIR Analysis

Figure 13 represents the FTIR spectra of the GBM (phosphate sludge + clay), GBD (sludge + diatomite), and GBDM (sludge + diatomite + metakaolin) series reveal distinct structural signatures. the Si–O–Si/Al band (1100–950 cm^{-1}) shifts to 980 cm^{-1} (GBM), 950 cm^{-1} (GBD), and 960 cm^{-1} (GBDM), reflecting differential Al incorporation into the silicate network [37,17]. The marked reduction of the 450 cm^{-1} band (Si–O) in GBDM indicates advanced consumption of clay phases [38], while residual peaks at 800 cm^{-1} (illite) [17] and 700 cm^{-1} (quartz) stabilize the matrix at high temperatures [39]. The hydroxyl region (3300–3600 cm^{-1}) shows increased residual porosity for GBD (linked to diatomite) and improved condensation for GBDM (via metakaolin) [40]. Compared to fly ash-based geopolymers (960 cm^{-1}, low hydroxyl absorption) or slag-based systems (dominant amorphous halo) [41]. These formulations combine residual crystalline phases and complete carbonate decomposition (1470 cm^{-1}) at 400 °C, offering superior thermal stability. The GBDM series, optimizing the Si/Al ratio

 doi:10.20944/preprints202506.1064.v1

through metakaolin, outperforms conventional geopolymers in structural stability and dehydration resistance, confirming the efficacy of hybrid systems [42].

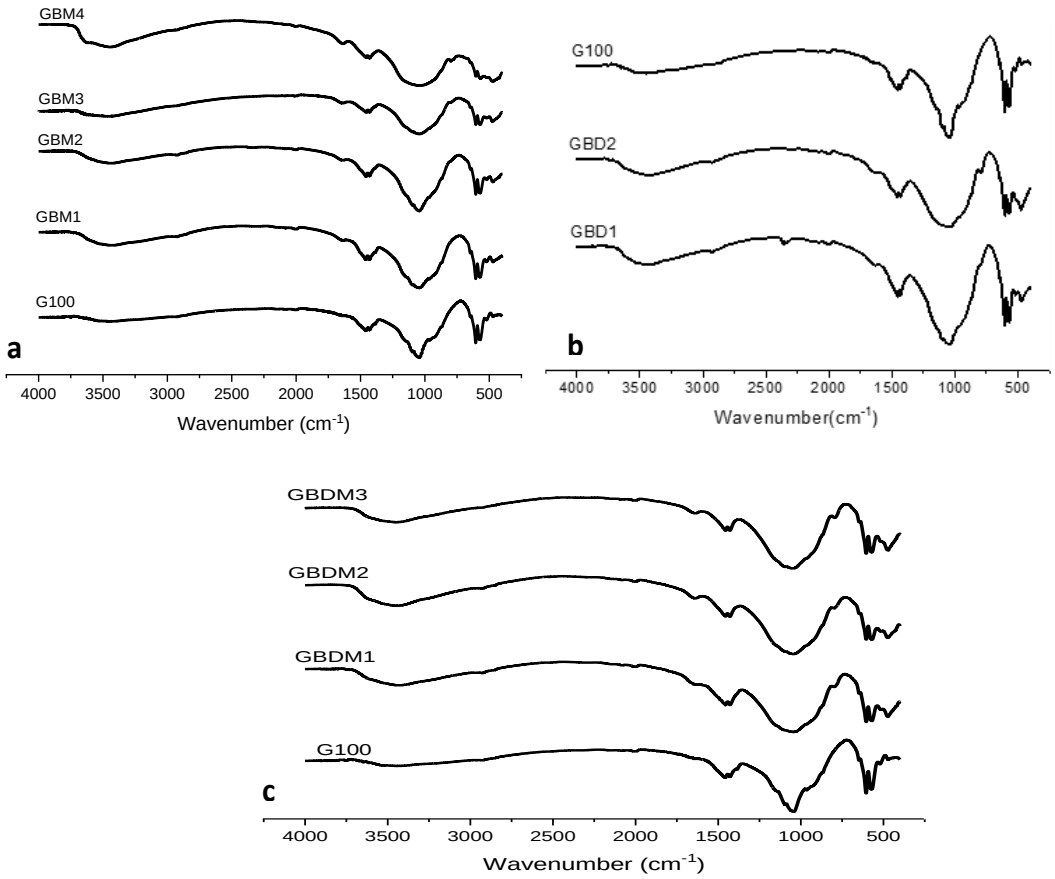

Figure 13. FTIR spectra of GBM serie (a) GBD series (b) and GBDM series (c) geopolymers.

Thermogravimetric Analysis

The study of the thermal behavior of synthesized geopolymer materials, based on the thermograms of the GBM, GBD, and GBDM series (Figures 14), highlights significant differences depending on the composition and treatment of the raw materials. For the GBM series, the main mass loss occurs between 25 and 600 °C, corresponding to the removal of free water, dehydroxylation of –OH groups, and decomposition of carbonates, with a moderate total mass loss (4–6%) (Figure 19), which could lead to higher porosity at elevated temperatures, indicating good consolidation of the geopolymer network [34];(Dabbebi et al., 2018). The GBD formulations (Figure 14) show contrasting behaviors: GBD1 is exceptionally stable, GBD2 combines low mass loss (~3%) and strong thermal robustness, while G100 (100% calcined phosphate sludge) exhibits a more pronounced mass loss due to carbonate decomposition [35]. Finally, The GBDM series, which incorporates calcined diatomite and clay, exhibits excellent thermal stability, with all samples losing less than 3% of their mass up to 1200 °C. Among them, GBDM2 stands out by offering the best compromise between minimal mass loss and structural robustness, making it particularly suitable for refractory applications. This superior performance is attributed to the optimized combination of calcined diatomite and clay, which enhances the formation of a dense, stable geopolymer network capable of withstanding high temperatures without significant degradation [26,40]. These results confirm the importance of initial composition and the use of calcined diatomite and clay to achieve lightweight, stable, and high-performance geopolymers at high temperatures.

 doi:10.20944/preprints202506.1064.v1

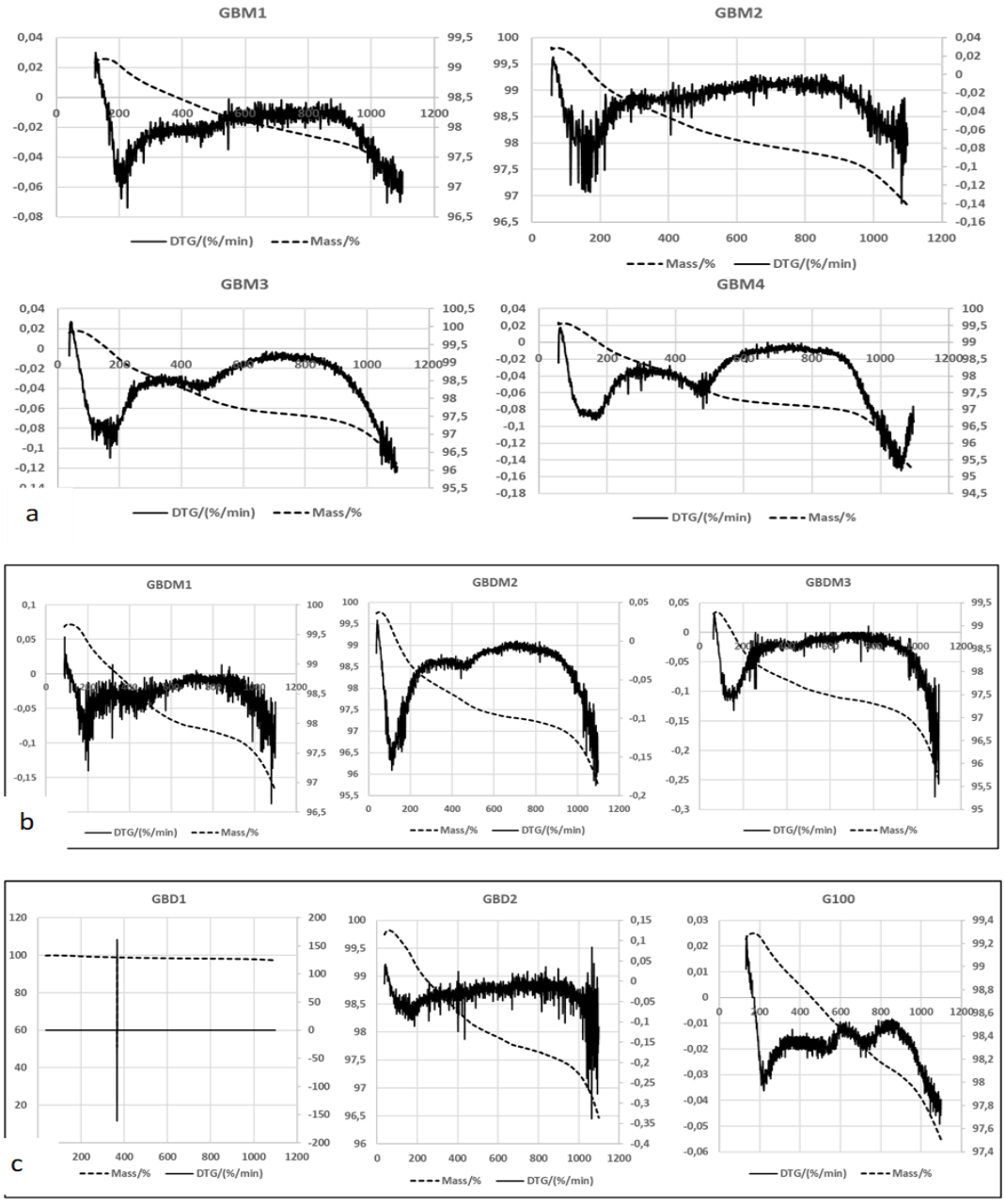

Figure 14. Thermal behavior of geopolymers: (a) GBM serie, (b): GBDM Serie and (c): GBD Serie.

Environmental Assessment of Heavy Metal and Anion Leaching from Geopolymer Formulations

Across all formulations in Table 4, most heavy metals remain well below ISDND limits, indicating effective immobilization within the geopolymer matrix. Sulfate, chloride, and fluoride levels are sometimes elevated (e.g., sulfate up to 1195 mg/L in GBDM1), but still comply with non-hazardous waste regulations.

Chromium (Cr) is the main limiting factor: in the formulations, its concentration ranges from 10 to 41 mg/L, exceeding both the inert (ISDI: 0.5 mg/L) and often the non-hazardous (ISDND: 10 mg/L) thresholds, but remaining below the hazardous waste limit (ISDD: 70 mg/L). This elevated Cr content is directly linked to the use of calcined phosphate sludge, which is very rich in leachable Cr. However, the reduction in Cr concentration compared to the pure calcined sludge is due to dilution effects and partial immobilization by the geopolymer matrix. To conclude, the geopolymer formulations can be

 doi:10.20944/preprints202506.1064.v1

classified as non-hazardous waste for most elements, but the Cr content remains above the thresholds for inert and non-hazardous waste, limiting their valorization without further treatment. Optimizing the formulation or adding specific stabilizing agents for chromium is recommended to improve environmental performance [43].

Table 4. heavy metals and anions of geopolymers.

Elements	GBM 1	GBM 2	GBM 3	GBM 4	GBD 1	GBD 2	GBDM 1	GBDM 2	GBDM 3	G100	ISDI	ISDND	ISDD
As	<0.1	<0.1	0.13	0.35	<0.1	0.12	<0.1	0.13	< 0.1	< 0.1	0.5	2	25
Ba	< 0.008	< 0.008	< 0.008	< 0.008	< 0.008	< 0.008	< 0.008	< 0.008	0.009	0.012	20	100	300
Cd	<0.009	<0.009	<0.009	<0.009	< 0.009	< 0.009	< 0.009	< 0.009	< 0.009	0.01	0.04	1	5
Cr	10	13	16	19	13	18	14	16	20	41	0.5	10	70
Cu	< 0.02	< 0.02	< 0.02	< 0.02	< 0.02	< 0.02	< 0.02	< 0.02	< 0.02	< 0.02	2	50	100
Mo	0.91	1.7	2.2	2.1	1.7	2.0	1.1	2.1	2.3	2.9	0.5	10	30
Ni	<0.05	< 0.05	< 0.05	< 0.05	< 0.05	< 0.05	< 0.05	< 0.05	< 0.05	< 0.05	0.4	10	40
Pb	<0.03	< 0.03	< 0.03	< 0.03	0.05	< 0.03	< 0.03	< 0.03	< 0.03	< 0.03	0.5	10	50
Sb	<0.09	0.10	0.10	0.08	0.09	0.12	0.065	< 0.06	0.079	0.18	0.06	0.7	5
Se	0.87	2.2	2.7	2.5	2.2	1.9	1.1	2.8	2.2	2.8	0.1	0.5	7
Zn	< 0.01	0.74	< 0.01	< 0.01	< 0.01	< 0.01	< 0.01	< 0.01	< 0.01	< 0.01	4	50	200
Sulfates	243	772	734	151	1033	841	298	1042	1100	595	1000	20000	50000
Chlorures	50	70	98	151	34	25	54.5	74.4	40.3	40.8	800	15000	25000
Fluorures	4.9	8.4	7.2	7.0	11	6.6	5.2	8.0	7.5	7.0	10	150	500

Conclusions

In this research, tunisian phosphate washing sludge undergoes significant structural and chemical transformations upon calcination at 850 °C, as evidenced by fluorescence X-ray, X-ray diffraction, FTIR, thermal, and particle size analyses. These modifications enhance the material's suitability as a precursor for geopolymer synthesis. The geopolymerization tests confirmed that phosphate sludge can be effectively valorized into geopolymers cured at ambient temperature, offering a sustainable alternative to traditional refractory materials.

The mechanical properties of the resulting geopolymers are strongly influenced by the precursor composition and alkaline activator concentration. Incorporating diatomite and kaolinitic clay, alongside optimizing potassium silicate content, notably improved the compressive strength and durability of the bricks. However, exceeding the optimal activator concentration adversely affected compressive strength, likely due to altered dissolution and gelation dynamics during geopolymer formation.

From an environmental perspective, this valorization approach aligns with principles of sustainability and circular economy by converting phosphate mining residues into valorized construction materials. This approach reduces waste storage volumes, mitigates soil and water contamination risks, and lowers the carbon footprint associated with conventional refractory brick production. Furthermore, the low-temperature curing of geopolymers significantly decreases energy consumption and greenhouse gas emissions associated.

 doi:10.20944/preprints202506.1064.v1

Overall, this work highlights the promising potential of phosphate washing waste as an eco-friendly raw material for producing durable, sustainable refractory bricks, thereby contributing to waste valorization and environmental preservation.

Future research should focus on scaling up the synthesis process, refining formulations for industrial application, and ensuring the safe management of trace elements such as chromium to mitigate potential environmental and health risks.

References

1. H. Idrissi *et al.*, "Sustainable use of phosphate waste rocks: From characterization to potential applications," *Mater Chem Phys*, vol. 260, p. 124119, Feb. 2021, doi: 10.1016/J.MATCHEMPHYS.2020.124119.
2. R. Hakkou, M. Benzaazoua, and B. Bussière, "Valorization of Phosphate Waste Rocks and Sludge from the Moroccan Phosphate Mines: Challenges and Perspectives," *Procedia Eng*, vol. 138, pp. 110–118, 2016, doi: 10.1016/j.proeng.2016.02.068.
3. M. Brahmi, S. Zouari, and M. Rossi, "L ' industrie minière et ses effets écologiques . État socio-économique et environnemental dans le bassin minier tunisien," pp. 109–120, 2019.
4. A. Bayoussef *et al.*, "Manufacturing of high-performance ceramics using clays by-product from phosphate mines," in *Materials Today: Proceedings*, Elsevier, Jan. 2020, pp. 3994–4000. doi: 10.1016/j.matpr.2020.10.800.
5. M. Ettoumi *et al.*, "Characterization of phosphate processing sludge from Tunisian mining basin and its potential valorization in fired bricks making," *J Clean Prod*, vol. 284, p. 124750, Feb. 2021, doi: 10.1016/J.JCLEPRO.2020.124750.
6. R. Obenaus-Emler, M. Falah, and M. Illikainen, "Assessment of mine tailings as precursors for alkali-activated materials for on-site applications," *Constr Build Mater*, vol. 246, p. 118470, Jun. 2020, doi: 10.1016/j.conbuildmat.2020.118470.
7. S. Moukannaa, M. Loutou, M. Benzaazoua, L. Vitola, J. Alami, and R. Hakkou, "Recycling of phosphate mine tailings for the production of geopolymers," *J Clean Prod*, vol. 185, pp. 891–903, 2018, doi: https://doi.org/10.1016/j.jclepro.2018.03.094.
8. R. Zeng, Y. Ge, W. Sun, X. Du, W. Chen, and G. Duan, "Method for purifying flotation phosphate tailings and preparing concrete blocks," Nov. 2019
9. F. Boutaleb, N. Boutaleb, S. Deblij, S. El Antri, and B. Bahlaouan, "Effect of Phosphate Mine Tailings from Morocco on the Mechanical Properties of Ceramic Tiles," *International Journal of Engineering Research and*, vol. 9, no. 02, Feb. 2020, doi: 10.17577/IJERTV9IS020092.
10. F. Z. Boutaleb, N. Boutaleb, B. Bahlaouan, D. Sanaa, and S. El Antri, "Production of ceramic tiles by combining Moroccan phosphate mine tailings with abundant local clays," *Mediterranean Journal of Chemistry*, vol. 10, no. 6, pp. 568–576, Jun. 2020, doi: 10.13171/MJC10602006221445NB.
11. M. A. Harech *et al.*, "From by-product to sustainable building material: Reusing phosphate washing sludge for eco-friendly red brick production," *Journal of building engineering*, vol. 78, pp. 107575–107575, Nov. 2023, doi: 10.1016/J.JOBE.2023.107575.
12. O. Inabi, A. Khalil, A. Zouine, R. Hakkou, M. Benzaazoua, and Y. Taha, "Investigation of the Innovative Combined Reuse of Phosphate Mine Waste Rock and Phosphate Washing Sludge to Produce Eco-Friendly Bricks," *Buildings*, vol. 14, no. 9, pp. 2600–2600, Aug. 2024, doi: 10.3390/BUILDINGS14092600.
13. M. P. Kulakowski, F. A. Brehm, C. A. M. Moraes, A. Pampanelli, and V. Reckziegel, "Monitoring and Evaluation of Industrial Production of Fired-Clay Masonry Bricks with 2.5% of Phosphatization Sludge," *Key Eng Mater*, vol. 634, pp. 206–213, Dec. 2014, doi: 10.4028/WWW.SCIENTIFIC.NET/KEM.634.206.
14. J. Muliawan and S. Astutiningsih, "Preparation and characterization of Phosphate-Sludge kaolin mixture for ceramics bricks," *International Journal of Technology*, vol. 9, no. 2, pp. 317–324, 2018, doi: 10.14716/ijtech.v9i2.1119.
15. R. Dabbebi, S. Baklouti, J. L. Barroso de Aguiar, F. Pacheco-Torgal, and B. Samet, "Investigations of geopolymeric mixtures based on phosphate washing waste," *Science and Technology of Materials*, vol. 30, pp. 1–5, Dec. 2018, doi: 10.1016/J.STMAT.2018.08.001.

 doi:10.20944/preprints202506.1064.v1

16. H. Baccour, H. Koubaa, and S. Baklouti, "Phosphate sludge from tunisian phosphate mines: Valorisation as ceramics products," *Advances in Science, Technology and Innovation*, pp. 1479–1480, 2018, doi: 10.1007/978-3-319-70548-4_431.
17. S. Mkaouar, "Valorisation de quelques formations argileuses pour la production de Briques en Terres Crues et de matériaux Géopolymères," 2021. [Online]. Available: http://www.theses.rnu.tn/fr/dynamique/uploads/cfd2b6661e8090e5e6f9672023c2d062.pdf
18. S. Louati, S. Baklouti, and B. Samet, "Geopolymers Based on Phosphoric Acid and Illito-Kaolinitic Clay," *Advances in Materials Science and Engineering*, vol. 2016, 2016, doi: 10.1155/2016/2359759.
19. R. Zheng, Z. Ren, H. Gao, A. Zhang, and Z. Bian, "Effects of calcination on silica phase transition in diatomite," *J Alloys Compd*, vol. 757, pp. 364–371, Aug. 2018, doi: 10.1016/J.JALLCOM.2018.05.010.
20. I. K. Ilia, M. G. Stamatakis, and T. S. Perraki, "Mineralogy and technical properties of clayey diatomites from north and central Greece," vol. 1, no. 4, 2009, doi: 10.2478/v10085-009-0034-3.
21. A. Tlili, R. Saidi, A. Fourati, N. Ammar, and F. Jamoussi, "Mineralogical study and properties of natural and flux calcined porcelanite from Gafsa-Metlaoui basin compared to diatomaceous filtration aids," *Appl Clay Sci*, vol. 62–63, pp. 47–57, Jul. 2012, doi: 10.1016/J.CLAY.2012.04.012.
22. "Moyens et méthodes pour améliorer la résistance à la compression de la brique réfractaire - Support technique - Zibo Jucos Co., Ltd," Zibo Jucos Co., Ltd. Accessed: Mar. 19, 2025. [Online]. Available: https://fr.jucosceramicfiber.com/info/ways-and-methods-of-improving-compressive-stre-48546449.html#
23. Y. Taha, "Valorisation des rejets miniers dans la fabrication de briques cuites : Évaluations technique et environnementale," 2017. doi: 10.13140/RG.2.2.19573.78565.
24. M. Amine, M. Mesnaoui, and Y. Abouliatim, "Effect of temperature and clay addition on the thermal behavior of phosphate sludge," *Boletín de la Sociedad Española de Cerámica y Vidrio*, vol. 60, no. 3, pp. 194–204, 2020, doi: 10.1016/j.bsecv.2020.03.002.
25. H. Hamdane *et al.*, "Effect of alkali-mixed content and thermally untreated phosphate sludge dosages on some properties of metakaolin based geopolymer material," *Mater Chem Phys*, 2020, doi: 10.1016/j.matchemphys.2020.122938.
26. M. Nykiel *et al.*, "The Influence of Diatomite Addition on the Properties of Geopolymers Based on Fly Ash and Metakaolin," pp. 1–18, 2024.
27. L. Chen, Z. Wang, Y. Wang, and J. Feng, "Preparation and properties of alkali activated metakaolin-based geopolymer," *Materials*, vol. 9, no. 9, Sep. 2016, doi: 10.3390/ma9090767.
28. Y. Chen, Y. Zhang, T. Chen, Y. Zhao, and S. Bao, "Preparation of eco-friendly construction bricks from hematite tailings," *Constr Build Mater*, vol. 25, no. 4, pp. 2107–2111, Apr. 2011, doi: 10.1016/J.CONBUILDMAT.2010.11.025.
29. D. Malkapuram, S. O. Ballari, S. Chinta, P. Rajasekaran, and B. Venkatesan, "Mechanical , water absorption , efflorescence , soundness and morphological analysis of hybrid brick composites," 2024, [Online]. Available: https://doi.org/10.1590/1517-7076-RMAT-2024-0179
30. C. Bories, M. E. Borredon, E. Vedrenne, and G. Vilarem, "Development of eco-friendly porous fired clay bricks using pore-forming agents: A review," *J Environ Manage*, vol. 143, pp. 186–196, Oct. 2014, doi: 10.1016/J.JENVMAN.2014.05.006.
31. N. Phonphuak, M. Teerakun, A. Srisuwan, P. Ruenruangrit, and P. Saraphirom, "The use of sawdust waste on physical properties and thermal conductivity of fired clay brick production," *International Journal of GEOMATE*, vol. 18, no. 69, pp. 24–29, 2020, doi: 10.21660/2020.69.5706.
32. Pouhet Raphaëlle, "phd Formulation and durability of metakaolin-based geopolymers," *HAL Open SCIENCE*, no. April, pp. 1–264, 2015, [Online]. Available: https://tel.archives-ouvertes.fr/tel-01297848%0Ahttps://tel.archives-ouvertes.fr/tel-01297848/file/2015TOU30085.pdf
33. S. Selmani *et al.*, "Physical–chemical characterization of Tunisian clays for the synthesis of geopolymers materials," *Journal of African Earth Sciences*, vol. 103, pp. 113–120, Mar. 2015, doi: 10.1016/J.JAFREARSCI.2014.12.009.
34. N. Essaidi, "Discipline : Matériaux Céramiques et Traitements de Surface Najet ESSAIDI Le 12 Décembre 2013 Formulation de liant aluminosilicaté de type géopolymère à base de différentes argiles Tunisiennes," 2013, [Online]. Available: https://cdn.unilim.fr/files/theses-doctorat/2013LIMO4030.pdf

 doi:10.20944/preprints202506.1064.v1

35. Z. H. Zhang, H. J. Zhu, C. H. Zhou, and H. Wang, "Geopolymer from kaolin in China: An overview," *Appl Clay Sci*, vol. 119, pp. 31–41, Jan. 2016, doi: 10.1016/J.CLAY.2015.04.023.
36. I. Luhar and S. Luhar, "A Comprehensive Review on Fly Ash-Based Geopolymer," *Journal of Composites Science*, vol. 6, no. 8, 2022, doi: 10.3390/jcs6080219.
37. L. Zeghichi and S. Benalia, "Les géopolymères : matières premières et influence des paramètres de composition: a review," *The Journal of Engineering and Exact Sciences*, vol. 9, no. 11, p. 18838, Dec. 2023, doi: 10.18540/jcecvl9iss11pp18838.
38. M. AHMED HASSEN and Z. ADDA BENIKHLEF, "Synthés et caractérisation de liant hydrauliques Présenté Par :" [Online]. Available: https://dspace.univ-temouchent.edu.dz/bitstream/123456789/4990/1/inbound3408018541411183319 - Mahmoud Ahmed.pdf
39. N. Essaidi, B. Samet, S. Baklouti, and S. Rossignol, "Feasibility of producing geopolymers from two different Tunisian clays before and after calcination at various temperatures," *Appl Clay Sci*, vol. 88–89, pp. 221–227, Feb. 2014, doi: 10.1016/J.CLAY.2013.12.006.
40. H. Tchakouté Kouamo, "Elaboration et caractérisation de ciments géopolymères à base de scories volcaniques," 2013. [Online]. Available: http://lopesphilippe.free.fr/CimentsGeopolymeresScoriesVolcaniquesTchakouteKouame2013.pdf
41. H. Cheng-yong, L. Yun-ming, M. Mustafa, and A. Bakri, "Thermal Resistance Variations of Fly Ash Geopolymers : Foaming Responses," no. November 2016, pp. 1–11, 2017, doi: 10.1038/srep45355.
42. M. E. L. Alouani, "En vue de l ' obtention du DOCTORAT Synthèse et caractérisation des matériaux inorganiques de type géopolymères à base de cendres volantes et de métakaolin : Application en génie de l ' environnement et génie civil," 2020.
43. X. Ren, F. Wang, X. He, and X. Hu, "Resistance and durability of fly ash based geopolymer for heavy metal immobilization: properties and mechanism," *RSC Adv*, vol. 14, no. 18, pp. 12580–12592, 2024, doi: 10.1039/d4ra00617h.